



Cite this: *Chem. Soc. Rev.*, 2016, 45, 3468

Received 31st July 2015

DOI: 10.1039/c5cs00597c

www.rsc.org/chemsocrev

## Hierarchy in inorganic membranes

Juergen Caro

Thin films of a few  $\mu\text{m}$  thickness for particle filtration and gas separation cannot be applied as self-supporting layers since they are mechanically insufficiently strong. Therefore, these top layers for particle filtration and gas separation are usually deposited on porous mechanically strong supports with a hierarchical pore structure. To reduce the pressure drop of a gas stream over the membrane and to ensure high fluxes in filtration and gas separation, the cross section of the support is usually asymmetric or graded with a small thickness of the layer with the smallest pore size called the top layer. Since the pressure drop over a capillary with radius  $r$  is  $\sim r^4$ , the layer with the smallest pore size should be as thin as possible. The disk-like planar supports are usually prepared by sequential tape casting which is an expensive technology. Tubular supports with a hierarchical cross section can be prepared in one step by hollow fiber spinning, double mantle spinning or centrifugal casting.

### 1 Why are inorganic membranes often hierarchical?

Inorganic – but also organic – membranes very often have an asymmetric or a graded hierarchical wall structure as shown in Fig. 1. The hierarchical disk-shaped planar membranes consist of a stack of layers of different pore sizes on a mechanically stable coarse support. Depending on the pore size of the top layer, such hierarchical stacks can be used (i) for particle filtration (micro, ultra and nano filtration with pore sizes up to 100 nm, 10 nm and 1 nm, respectively) and (ii) for gas separation with an additional molecular sieve top layer (zeolite,

MOF, carbon... with pores in the Å-region) or a non-porous dense gas-selective top layer (perovskites, ionic liquids, polymers).

However, also hollow fiber membranes – produced by spinning technologies – can show a hierarchical cross section of their porosity as shown in Fig. 2. By tuning the parameters of the spinning process, the graded asymmetrical pore structure can be obtained. Other concepts to prepare membranes with a hierarchical cross section are double mantle spinning (Fig. 3) or centrifugal casting (Fig. 7).

Liquid filtration is achieved by porous organic or inorganic membranes with pore sizes larger than 1 nm. To reduce the flow resistance, the top filtration layer is relatively thin. Since this layer is not self-supporting, it is deposited on a mechanically strong wide-pore coarse support which results in a hierarchical cross section. The advantage of inorganic filter materials is their thermal stability, fouled membranes can be regenerated by oxidative thermal and chemical treatment. Inorganic membranes do not swell in organic vapors or solvents, they can be sterilized. Ceramic filter membranes can have a relatively narrow pore size distribution which gives a sharp cut-off which will be discussed in Section 2.

Gas separation by membrane permeation can be very energy-efficient and it usually requires less investment costs than the competing technologies such as pressure swing adsorption and cryogenic distillation. Correspondingly, permeation technologies have been developed for e.g. nitrogen production and hydrogen recovery which are based on organic polymer membranes. The separation factor of these organic polymer membranes is typically located in a moderate range, of around 5 up to 10, but rarely higher than 20. Inorganic porous and non-porous membranes can show much higher selectivities. Three examples of inorganic

*Institute of Physical Chemistry and Electrochemistry, Leibniz University Hannover, Callinstr. 3A, 30165 Hannover, Germany. E-mail: juergen.caro@pci.uni-hannover.de*



**Juergen Caro**

*Juergen Caro (1951) studied chemistry and obtained PhD at Leipzig University in 1977. Since 2001 he has been the chair of Physical Chemistry at Hannover University. J. Caro is author of about 300 publications and 38 patents. He is a visiting professor at the Chinese Academy of Sciences and at the Dalian University of Technology. He received in 2013 the Breck Award of the International Zeolite Association and the Ostwald Medal of the Saxonian Academy of Sciences.*

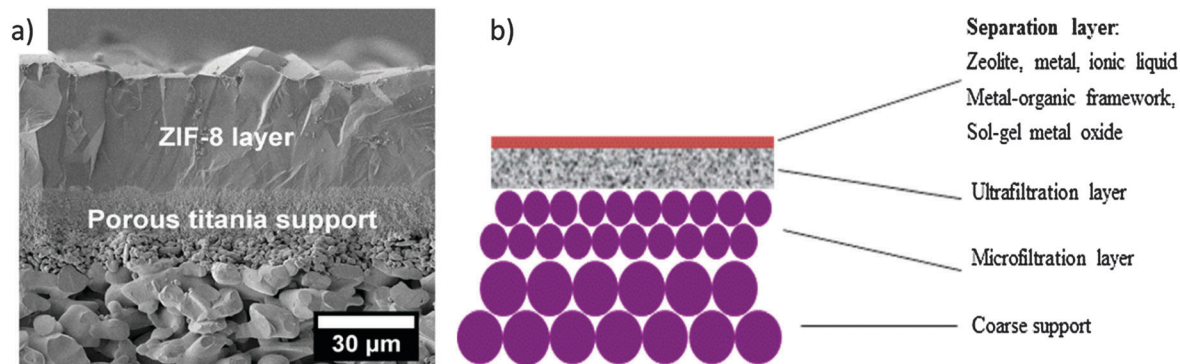


**Fig. 1** Typical planar ceramic membranes obtained by sequential tape casting with a gas selective layer on top. (a) A metal–organic framework (MOF) type ZIF-8 layer on an asymmetric graded titania support,<sup>1</sup> (b) principle of a supported membrane: the  $\mu\text{m}$ -thick separation layer is deposited on a macroporous ceramic or metallic support. To reduce the pressure drop across the support, *i.e.* to minimize the flow resistance, usually asymmetric (graded) supports with hierarchical cross section are used.

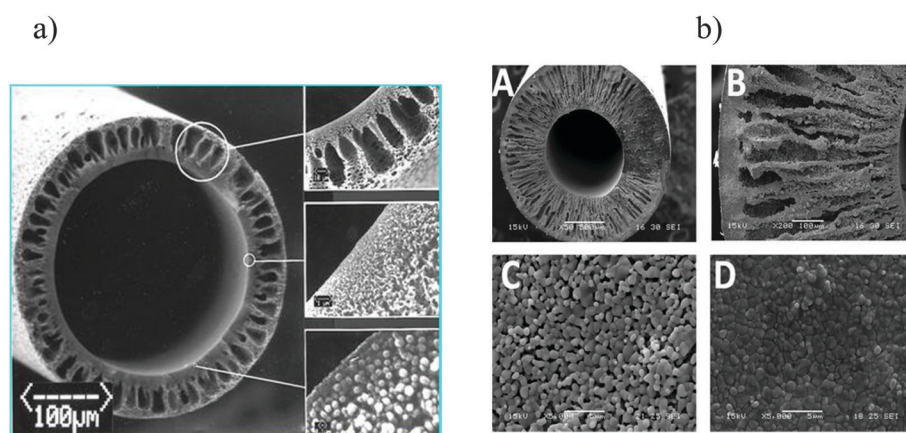


**Fig. 2** Typical organic and inorganic hollow fiber membranes with a hierarchical cross section. In (a) and (b), the hierarchical wall structure is obtained by tuning the parameters of the phase inversion spinning. (a) Polysulfon hollow fiber membranes for controlled insulin release.<sup>2</sup> (b) Alumina hollow fiber membrane with an asymmetric hierarchical cross section obtained by spinning. (A) Entire and (B) partial cross section, (C) inner and (D) outer surface.<sup>3</sup> Reproduced with permission from the American Chemical Society.

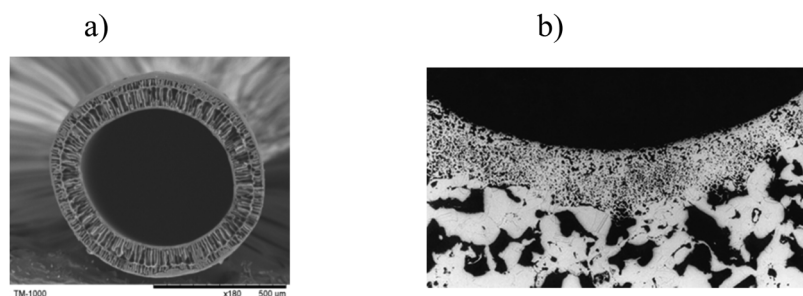


**Fig. 3** The hierarchical structure is produced by double mantle spinning. (a) Double mantle spun polylactide hollow fiber membranes for the use in hemodialysis.<sup>4</sup> (b) Sintered metal membranes that combine high permeability and very low pressure drop, yet retaining all the advantages of sintered metal filters.<sup>5</sup>

gas separation membranes with a hierarchical cross section are discussed in Section 3: zeolites, MOFs, and perovskites.

The organic polymers can be easily fabricated as cheap and flexible hollow fibers or spiral wound (plate and frame) membranes which is an important advantage of organic over inorganic membranes. However, (i) their selectivities are rather moderate, (ii) they

can be damaged or even destroyed by solvents, and (iii) they are not thermally stable at temperatures necessary for regeneration by calcinations (combustion of the organic residues). Inorganic membranes like porous metals, carbons or metal oxides do not show these disadvantages. However, they suffer from brittleness, thermal expansion problems and relatively high production costs.

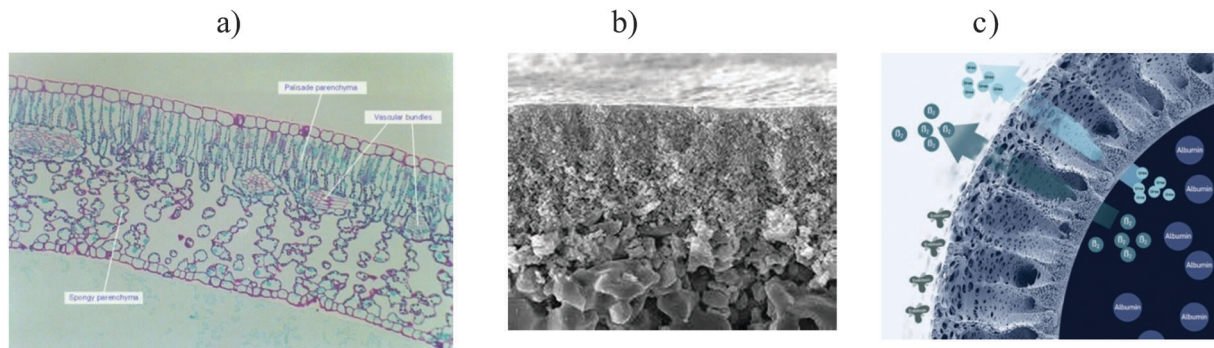


Fig. 4 Nature-inspired hierarchical membrane structures. (a) Cross section of a privet leaf.<sup>8</sup> (b) Fracture of a commercial TiO<sub>2</sub> ultrafiltration membrane of the company inopor.<sup>9</sup> (c) Cross section of a commercial blood hemodialysis membrane of Gambro's Polyflux Revaclear dialyzers.<sup>10</sup> The main components separated are urea and  $\beta_2$  (beta-2-microglobulin is a large molecule with a molecular weight of about 11 600 Daltons).

To minimize the flow resistance, *i.e.* to minimize the pressure drop over the membrane, the supports are of hierarchical structure. This hierarchical structure – as shown in Fig. 1–3 – is also called graded or asymmetric. The pressure drop over a porous layer is larger the smaller the pore diameters are, the layer thickness in a hierarchical membrane becomes smaller in the direction of the small pore layers. Besides the pressure drop, there is another practical reason to build graded asymmetric structures. The layers are deposited consecutively, *i.e.* layer-by-layer. First the coarse layer is deposited, followed by a micro-filtration layer, an ultrafiltration layer and finally a nano filtration and top layer (zeolite, MOF, carbon, metal) which give the selectivity. Becoming increasingly smaller in the pore size it can be avoided that in a certain deposition step the slurry to be deposited, which infiltrates the pores of the previous layer thus blocking them. Also for the deposition of the gas selective top layer it is advantageous if this layer does not penetrate the graded support thus blocking the transport pores.

It has to be noted that the development of membranes with a hierarchical cross section is nature-inspired. Fig. 4 shows the cross section of a privet leaf, of a planar commercial TiO<sub>2</sub> ultra filtration membrane and of a hollow fiber polymer membrane. Biology often uses hierarchical networks to bridge scales and

facilitate transport.<sup>6</sup> In the context of chemical engineering, this approach is called nature-inspired chemical engineering (NICE).<sup>7</sup>

During the last few years, numerous inorganic membranes with a hierarchical cross section have been developed not only zeolite and MOF but also supported metal and carbon membranes such as shown in Fig. 5.

In his contribution to this issue of *Chem. Soc. Rev.*, W. Schwieger gives a clear definition of hierarchical materials (Fig. 6). It follows from Fig. 6 that supported membranes as shown in Fig. 1–5 fulfill the definition of Type I hierarchical materials.

As mentioned above, the selective separation layer is in general deposited on one or several supporting layers having larger pores. For the sake of simplicity the mass transfer through such composites is frequently modelled using integral parameters. However, this simplified description has serious limitations, *e.g.* it is not capable of quantifying the often observed effects of direction dependencies of flow and selectivity. In ref. 14 the mass transfer is studied simultaneously to the production process of asymmetric membranes. The dusty gas model was capable of describing the overall transport in a wide parameter range for both flow directions.

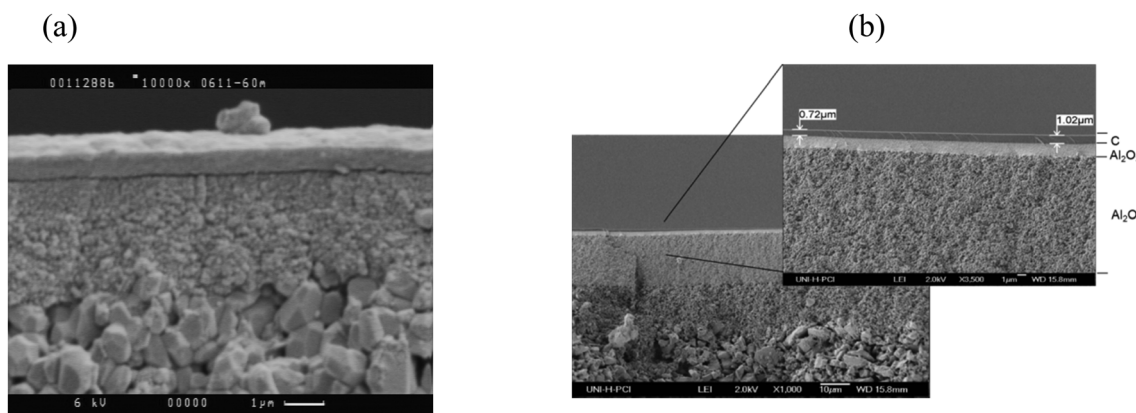


Fig. 5 Examples of inorganic membranes with a hierarchical cross section. (a) 0.6  $\mu\text{m}$  Ag/Pd (23% Ag) membrane on a ceramic support obtained by current less plating.<sup>11</sup> (b) An about 1  $\mu\text{m}$  carbon layer on top of a ceramic support obtained by pyrolysis of a polymer blend.<sup>12</sup>

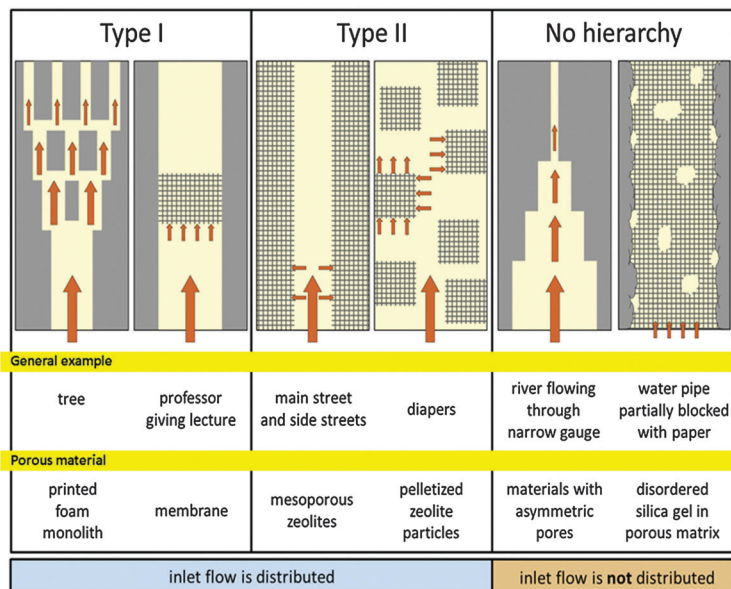


Fig. 6 Hierarchical materials after Schwieger *et al.*<sup>13</sup> Reproduced with permission from the Royal Society of Chemistry.

The asymmetric, *i.e.* graded cross section structure of the supported molecular sieve membranes justifies to regard them as hierarchical materials of Type I following Fig. 7. On the other hand, this hierarchical layered structure as shown in Fig. 1–5 is responsible for the high costs of zeolite or MOF membranes prepared on hierarchical porous ceramic supports. About 80–90% of the costs of a zeolite membrane are contributed to the graded tubular or planar ceramic (alumina, zirconia, titania...) support.<sup>15</sup> These costs are mainly due to the fact that after coating each layer, a firing step has to follow before the next layer can be coated which has to be fired again. Therefore, different concepts are followed for a one-step cheap preparation of hierarchical supports. One of the concepts is centrifugal casting or rotocasting. This technique is typically used to cast thin-walled metallic cylinders. A molten metal is centrifugally thrown against the inside mold wall at a high speed (300–3000 rpm) where it solidifies after cooling. The technique of centrifugal casting can be applied also to produce in one step

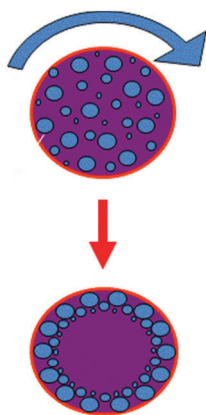


Fig. 7 Principle of centrifugal casting to get tubes with a hierarchical wall structure in one step.<sup>19</sup>

tubular membranes with a hierarchical wall structure,<sup>16–18</sup> as shown schematically in Fig. 7. Tubes can be produced easily by centrifugal casting of a weakly coagulated aqueous slurry in rotating tubular molds under accelerations between 20 and 100 times of gravitational acceleration. Note that in this technique a slightly polydisperse suspension has to be taken.

## 2 Case study one: use of pore membranes with a hierarchical pore structure in filtration

Since inorganic membranes are stable against swelling by organic feeds and solvent molecules, they can be used properly in filtration. Further, ceramics are hydrophilic and, therefore, especially water can be transported. Fig. 8 shows a TiO<sub>2</sub> ultra-filtration membrane which is used in the dye works industry for the recovery of dye from waste water. Fig. 9 gives an overview over micro ultra and nano filtration membranes. Table 1 shows the separation performance of the micro, ultra and nano

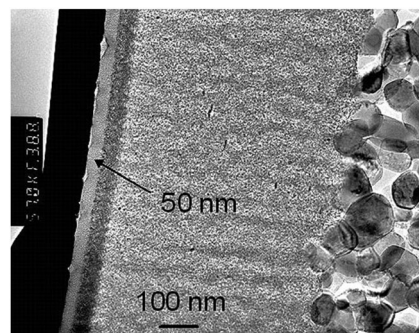


Fig. 8 Graded TiO<sub>2</sub> high-flux nano filtration membrane with a cut-off of 15 Å as it is used for the recovery of dyes from waste water in the textile industry.<sup>20</sup>

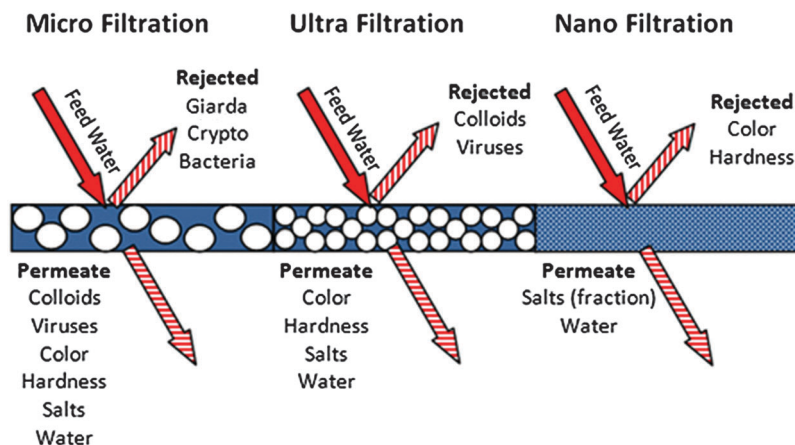


Fig. 9 The three membrane filtration processes: micro (MF), ultra (UF) and nano (NF) filtration.<sup>21</sup>

Table 1 Hierarchy of particle filtration membranes

Process	Micro filtration (MF)	Ultra filtration (UF)	Nano filtration (NF)
Pore size	1–0.1 $\mu\text{m}$	100–2 nm	<2 nm
Objects separated	Microorganisms, plankton, bacteria algae, suspended solids, oil–water emulsions	Viruses, colloids, macromolecules, milk protein, gelatin, protein fractionation, milk and whey fractionation	Large ions, dissolved organic carbon (DOC), large hydrated ions, demineralization

filtration membranes. Fig. 10 shows as an example that filtration membranes with ceramic nano-, ultra- and micro-filtration top layers can have relatively sharp pore size distributions in comparison with organic porous membranes.

As stated above, the main reason to build hierarchical pore structures is to minimize the pressure drop over the porous membranes. The volumetric flow  $F$  ( $\text{m}^3 \text{s}^{-1}$ ) through a capillary is described by the well-known Hagen–Poiseuille equation (eqn (1)) which gives the pressure drop  $\Delta P$  in an incompressible and Newtonian fluid of viscosity  $\eta$  (Pa s) in laminar flow flowing through a cylindrical capillary of length  $L$  of constant radius  $r$ .

$$\Delta P = \frac{8\eta LF}{\pi r^4} \quad (1)$$

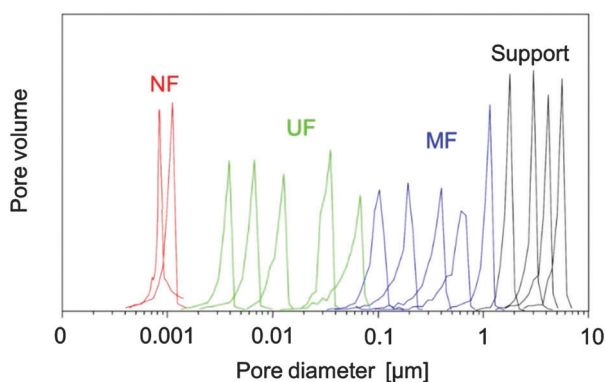


Fig. 10 Pore size distribution for several commercial nano filtration (NF), ultra filtration (UF) and micro filtration (MF) membranes as well as several supports of inopor GmbH.<sup>9</sup>

In other words, the volumetric flow  $F$  is proportional  $\Delta P \cdot r^4 \cdot L^{-1}$ . We have to note that eqn (1) describes the volumetric flow through one capillary. For the calculation of such membrane parameters like flux density ( $F$  per area) or permeance ( $F$  per area and pressure difference over the membrane), we have to consider the pore density per membrane area.

By a hierarchical structure, in ref. 22 polysulfone, polyvinylpyrrolidone or blends of these polymers with enhanced fluxes for the separation of oil-water nano-emulsions have been developed. The challenge of this membrane development can be described as follows: the thin nanoporous layer is necessary for the high selectivity but it is linked to a high pressure drop, while the thick microporous layer yields high flow rates with low flux resistance and pressure drop, giving the mechanical stability. The thickness of the microporous layer must be sufficient to render the membrane mechanically robust. However, the thickness and the pore size of the nanoporous layer must be carefully optimized since especially the pressure drop  $\Delta P$  and the volumetric flow  $F$  depend on the pore size  $r^4$ . The aim is to find out the maximum flow rate while still rejecting the water droplets. The optimized hierarchical membrane structure is shown in Fig. 11.

However, the Hagen–Poiseuille law (eqn (1)) describes the volumetric flow ( $V$  in  $\text{m}^3 \text{s}^{-1}$ ) through one capillary – or normalized per membrane area – the volumetric flow through an ensemble of parallel straight capillaries. Since real filter membranes consist of a hierarchical system of branched pores (as shown in Fig. 12), the bifurcation angle becomes an important parameter. By using computational fluid dynamic simulations in ref. 23 the effect of the porosity, pore size, and the bifurcation angle on the fluid behavior and pressure drop

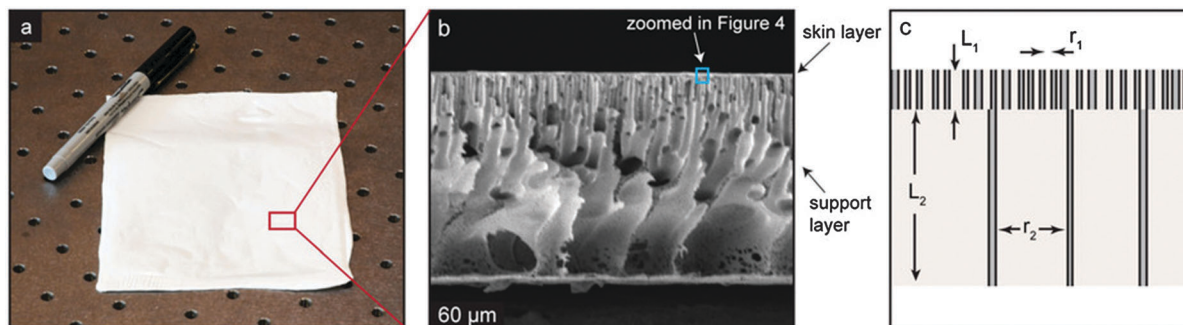


Fig. 11 Image and schematic of hierarchical membranes. (a) Photo of the polysulfone membrane. (b) SEM of the cross section of PSf membranes showing the hierarchical geometry featuring a skin layer. (c) Idealized schematic of a hierarchical membrane showing a skin layer with small pores and a support layer with larger pores.<sup>22</sup>

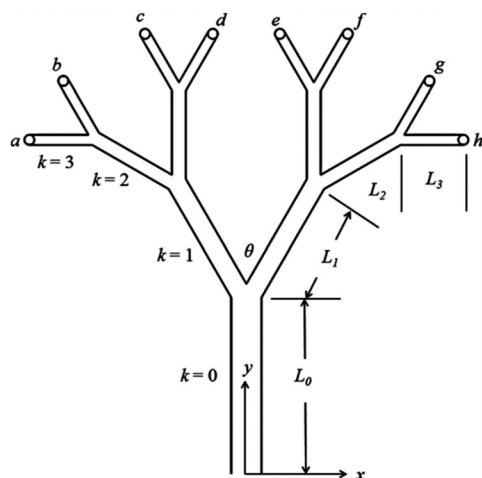


Fig. 12 Nomenclature and coordinate system for branching flow networks. The numbers  $k = 0 \dots 3$  indicate the  $k$ th order branch (reproduced from ref. 23 with permission).

for flow networks with hierarchical bifurcation flow passage as shown in Fig. 12 has been studied. The amount of fluid that travels through the tree-like membrane before passing through the porous disks is highly dependent on the bifurcation angle. The effect of the bifurcation angle on pressure drop was found to be highly dependent on the porosity and pore size. The bifurcation angle had the greatest impact on pressure drop at low porosities and small pore sizes.

### 3 Case study two: gas separation membranes with a hierarchical cross section

The top layer of the particle filter membranes with the smallest pore size as discussed in the previous section is about 1 nm for nano filtration. This pore size allows Knudsen separation of gas mixtures but no molecular sieving. Therefore, another gas-selective top layer has to be brought on the graded asymmetric wall, a permselective porous (zeolite, metal-organic framework (MOF)) or dense (perovskite).

#### 3.1 Zeolite membranes with a hierarchical structure

The state of the art of zeolite membrane preparation, characterization, permeative testing and industrial application is just recently reported in ref. 24. As an example, Fig. 13 shows a supported ZSM-5 layer on a graded asymmetric titania support giving a pore membrane with a hierarchical pore structure. It is interesting to note that in this special case titania instead of alumina supports have been selected to avoid any acid sites on the silicalite I (Al-free ZSM-5) top layer since this membrane was designated for olefin separation.<sup>25</sup>

Often, an orientation of the grown top layer zeolite film can be stated from the comparison of the powder XRD with the XRD of the supported zeolite film. Fig. 14 gives 2 examples.

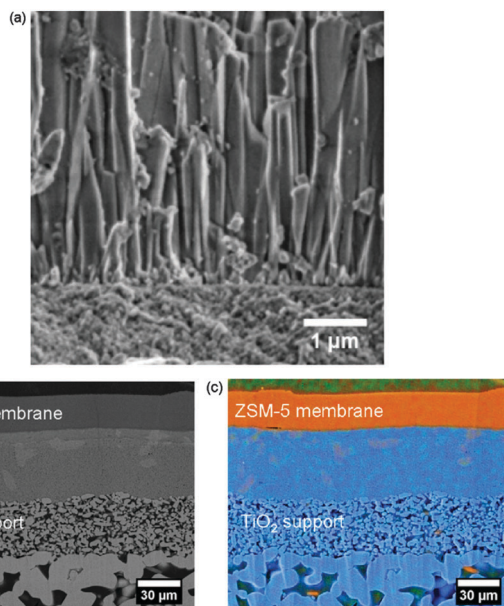


Fig. 13 SEM images of the cross section of a supported ZSM-5 membrane on a hierarchical  $\text{TiO}_2$  support. The cross section shown in (a) was simply broken. (b) A cross section polished with Ar ions. Energy dispersive X-ray spectroscopy (EDXS) shown in (c) was applied to identify the element distribution: Si in orange, Ti in turquoise.<sup>26</sup> Reproduced with permission from Elsevier.

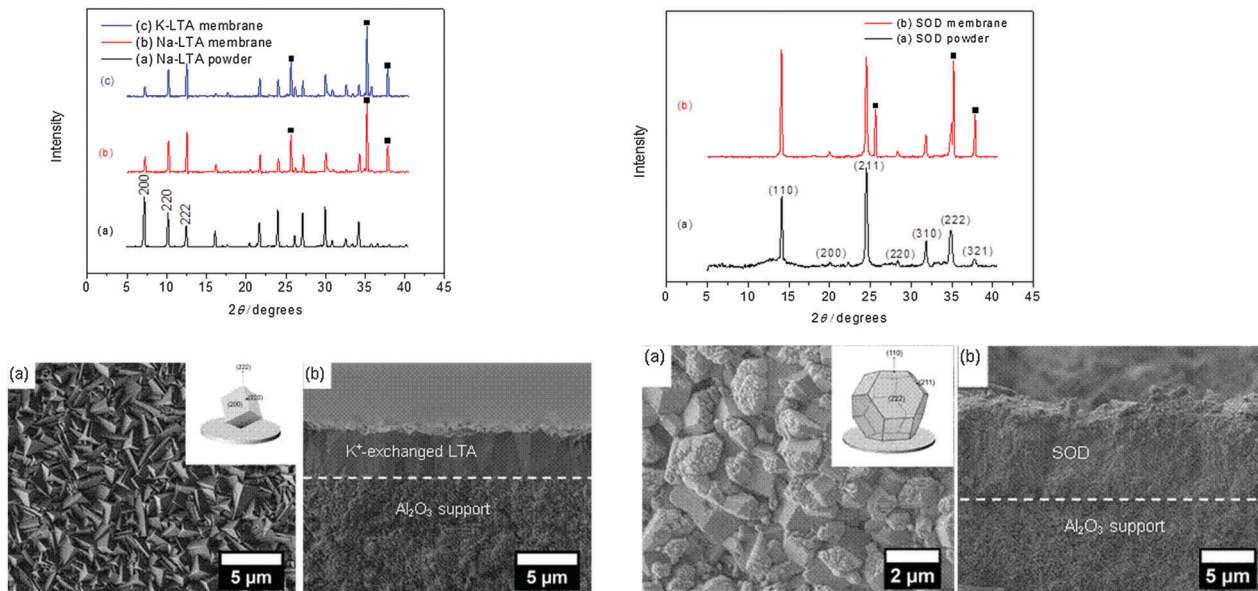


Fig. 14 Powder XRD and SEM (top view with crystal orientation) and cross section as deduced from comparing the XRD of the powder with the supported layer: LTA (left) and SOD (right).<sup>27</sup> Reproduced with permission from Elsevier.

Zeolite membranes match very well with ceramic or metal supports since (i) most zeolite structures are prepared by means of a structure-directing agent (SDA), also called the template. The organic SDA molecules become incorporated during zeolite crystallization into the zeolite lattice and have to be removed before zeolite application by thermal calcination in air at about 500 °C. (ii) Some zeolite structures like LTA, FAU and to some extent MFI can be prepared without SDA, but also in this case inorganic supports are necessary for the thermally-oxidative regeneration of zeolite membranes blocked by accumulated traces of high-boiling impurities. However, if the graded asymmetric structure of the ceramic support is produced by sequential tape casting, the costs of the supported zeolite membrane are dominated by the support and not by the zeolite film.<sup>28</sup> Therefore, zeolite membrane costs are a major factor to be considered for industrial applications. An estimated price limit of membranes for petrochemical applications is €200 m<sup>-2</sup>.<sup>29,30</sup> In contrast, at present the prices for zeolite membranes are estimated to be close to €1.000 m<sup>-2</sup>. For comparison: the price of a typical polymer membrane in flat geometry is approximately €10 m<sup>-2</sup> hollow fibers are approximately €5 m<sup>-2</sup>.<sup>31</sup> Although the manufacture of inorganic membranes is more expensive than the production of polymeric ones, the long-term cost implications due to their chemical and thermal stability make the use of inorganic membranes a viable option. A reduction of the prices of zeolite membranes can be expected by using honeycomb substrates with a higher membrane area per membrane element.

### 3.2 Metal-organic framework (MOF) membranes with a hierarchical structure

There are some intrinsic properties of MOFs in comparison with zeolites, which allow an easy and cheap synthesis:

- Most MOFs can be formed at low, even room temperature, by repeated dipping of a substrate in linker and metal solutions.
- The linker molecule of a MOF allows chemical functionalization which enables a covalent link of a MOF to the substrate or to attach seed crystals to the substrate surface.
- After synthesis, MOFs contain only solvent molecules in their pore system which can be removed by evacuation at soft temperatures (<100 °C) thus allowing the formation of MOF layers on organic substrates.

As shown in case study one, there is some progress in the development of zeolite membranes. However, especially the long-term stability, T-cycling, regeneration and the difficult housing have prevented so far a major industrial use of zeolite membranes. Nevertheless, there is a healthy optimism that MOFs as a new star at the sky of nanoporous materials can solve these problems.<sup>32</sup> As hybrid organic-inorganic materials, MOFs consist of metal cations or cationic oxide clusters that are linked by organic molecules thus forming a crystalline network. MOFs, often also termed as coordination polymers. As a coordination network, the MOFs are mechanically less stiff and brittle as zeolites.<sup>33</sup> Therefore, MOFs frequently show a high degree of framework flexibility, which results in effects such as “breathing”, “gate opening” and “linker dynamics”.<sup>34</sup>

All the tools from the preparation of supported zeolite membranes such as seeding, microwave heating, ceramic porous supports, or intergrowth-supporting additives can be applied for the synthesis of MOF membranes. The organic linker molecules have high potential for specific functionalization allowing (i) the tuning of adsorptive interaction and (ii) the control of the pore size and accessible pore volume *via* the size of the functional groups.

Therefore, in a relatively short time the first MOF membranes with molecular sieve properties have been developed.

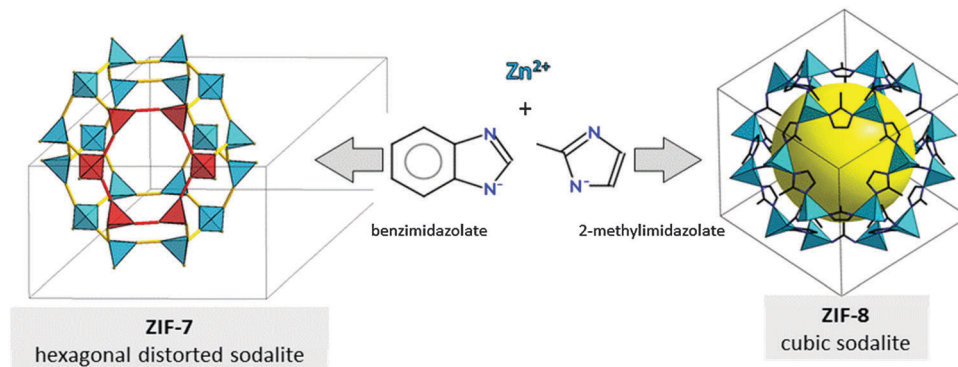


Fig. 15 SOD frameworks of ZIF-7 and ZIF-8.

Highlights are the highly permeable ZIF-8 membranes for  $CO_2/CH_4$  separation,<sup>35</sup> the copper-net supported HKUST-1 membranes with  $H_2/N_2$  selectivity of about 7,<sup>36</sup> the  $Co_3(HCOO)_6$  membranes with a  $CO_2/CH_4$  selectivity of up to 16,<sup>37</sup> a small pore MOF with a 0.32 nm pore size for  $H_2/N_2$  separation on alumina supports,<sup>38</sup> or the supported ZIF-69 membrane with a broad selectivity for different gas mixtures.<sup>39</sup> However, these MOF membranes show still a lower  $CO_2/CH_4$  selectivity than the best zeolite membranes SAPO-34<sup>40</sup> and DDR<sup>41</sup> membranes with separation factors above 115 and 4000, respectively. In our group we developed ZIF-7,<sup>42</sup> ZIF-8,<sup>43</sup> ZIF-22,<sup>44</sup> and ZIF-90<sup>45</sup> membranes for the molecular sieving of hydrogen. These ZIF membranes have been operated up to 200 °C and they were found to be stable at this temperature even in the presence of up to 3 vol% steam.

The zeolitic imidazolate frameworks (ZIFs) form a sub-family of MOFs. In ZIFs, metal cations (e.g.  $Zn^{2+}$ ,  $Co^{2+}$ ,  $Cu^{2+}$ ) are tetrahedrally coordinated by imidazolate linkers frequently resulting in a relatively thermally and hydrothermally stable network showing zeolite topologies. A well-known ZIF structure is ZIF-8, in which 2-methylimidazolite anions are linked to  $Zn^{2+}$  cations resulting in an expanded SOD structure. Another well-known MOF structure is ZIF-7 where the  $Zn^{2+}$  ions are interconnected by benzimidazolite anions (Fig. 15).

Fig. 16 shows a typical cross section of a supported ZIF membrane with “molecular sieving” properties. The MOF layer

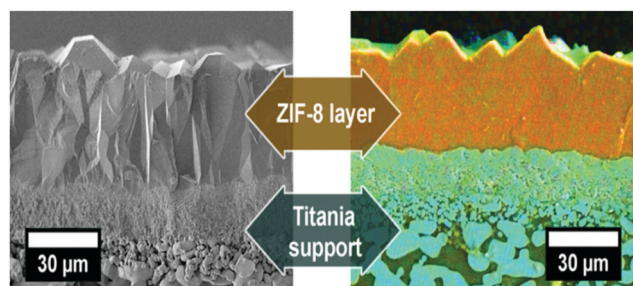


Fig. 16 Cross section of a ZIF-8 membrane on a macroporous titania support. Left: Scanning electron microscopy. Right: Energy dispersive X-ray spectroscopy (EDXS) in mapping mode, the element Zn is in orange and the element Ti in cyan showing the sharp transition between MOF layer and support.<sup>43</sup> Reproduced with permission from the American Chemical Society.

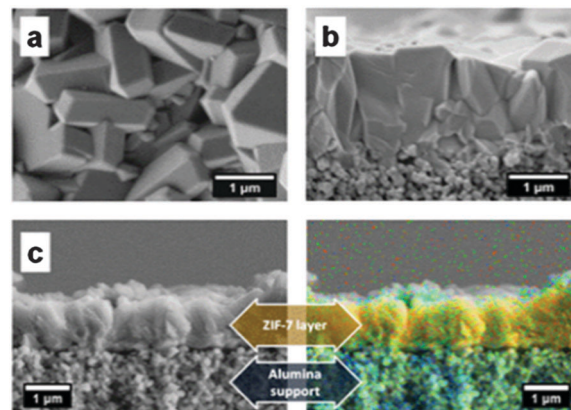


Fig. 17 About 1 μm thin MOF ZIF-7 layer on an alumina support prepared by seeding (secondary growth) in combination with microwave heating.<sup>46</sup> Reproduced with permission from Wiley-VCH.

was relatively thick (30 μm). By applying seeding in combination with microwave heating, the ZIF layer could be reduced to about 1 μm as shown in Fig. 17.

The concept of this widely used technique consists in the decoupling of (i) nucleation and seed formation at high supersaturation, and (ii) growth of the seed crystals to a continuous layer at low supersaturation. Usually, in the crystal growth step a new nucleation can be avoided and only the seeds grow to the molecular sieve layer. Therefore, the layers obtained by secondary growth are less polycrystalline.

Provided that the support surface is covered by a homogeneous and dense seed layer, relatively thin zeolite and MOF layers can be obtained. This seeding or secondary growth technique can be combined with a quick heating up of the autoclaves by microwaves. In the case of microwave heating, a new nucleation at heterogeneous surfaces (support, autoclave walls) is kinetically suppressed by the quick heating up, and only the seeds grow to the layer. As an example, Fig. 17 shows that an about 1 μm thin supported ZIF-7 molecular sieve layer could be obtained by combined seeding and microwave heating.

In the above examples, the gas-selective MOF layer has been crystallized on top of a graded asymmetric ceramic support. Since MOFs contain after crystallization no structure-directing



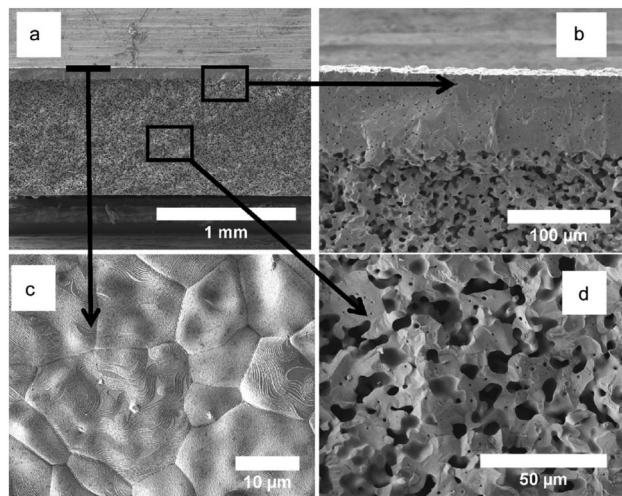


Fig. 18 SEM micrographs of the BSCF membrane: (a) overview of the membrane, (b) cross section of the dense BSCF part, (c) surface of the dense BSCF side, (d) cross section of the porous BSCF part which acts as support for the dense part.<sup>67</sup> Reproduced with permission from Elsevier.

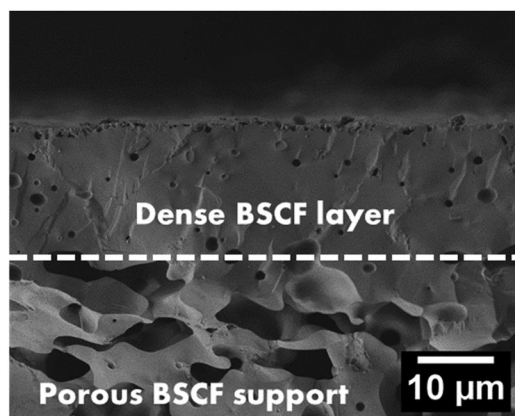


Fig. 19 Cross section of the high-flux  $\text{Ba}_{0.5}\text{Sr}_{0.5}\text{Co}_{0.8}\text{Fe}_{0.2}\text{O}_{3-\delta}$  (BSCF) perovskite membrane developed at FZ Juelich. The black spots in the top layer indicate a harmless closed porosity.<sup>71</sup> Reproduced with permission from Wiley-VCH.

agent (SDA) but only solvent molecules, MOFs can be activated for adsorption or permeation by heating at reduced pressure or

under a sweep gas to temperatures 100–200 °C. Therefore, MOFs can be grown on polymeric supports that can stand this mild activation. On the other hand, the thermal-oxidative regeneration of blocked MOF membranes (*e.g.* by high-molecular residues) is not possible. There are novel low-temperature synthesis strategies for MOF membrane layers.

Some commonly used approaches for MOF thin films preparation are growth from solvothermal mother solutions (using self-assembled monolayers, SAMs),<sup>47–49</sup> colloidal deposition, layer-by-layer or liquid phase epitaxy of SURMOFs,<sup>50–54</sup> electrochemical synthesis,<sup>55–58</sup> evaporation induced crystallization gel-layer synthesis and microwave-induced thermal deposition.<sup>59,60</sup>

If a porous support separates an aqueous and an organic solvent, one of the solvents contains the metal ion, the other the linker molecule, then a MOF layer forms at the contact zone polymer support – aqueous solvent<sup>61,62</sup> or inorganic support – organic solvent.<sup>63</sup> Recently, a scalable and inexpensive concept for processing MOF membranes in polymeric hollow fibers has been developed.<sup>64</sup>

In the layer-by-layer (LbL) deposition technique,<sup>65</sup> a support is repeatedly dipped into a solvent containing metal ions or linker molecules with a washing step in-between. Recently a spraying technique for the deposition of MOF layers on solid surfaces has been reported.<sup>66</sup>

### 3.3 Oxygen transporting perovskite membranes with a hierarchical structure

The concept of hierarchical structures to have high fluxes through reduced transport resistances has also been applied for oxygen-transporting perovskite-like membranes. Note that in this case the oxygen-selective top layer must be dense, whereas the support shows a porous structure to facilitate gas transport. As an example, the asymmetric  $\text{Ba}_{0.5}\text{Sr}_{0.5}\text{Co}_{0.8}\text{Fe}_{0.2}\text{O}_{3-\delta}$  (BSCF) perovskite oxygen transporting membranes consist of a dense oxygen separation layer on a porous BSCF support layer. Both layers were manufactured by tape casting using a BSCF powder, which provides perfect chemical compatibility and the same thermal expansion of the two layers. Two different slurries were prepared for the membrane layer and support layer. The slurry for the support layer contained 20 wt% corn starch in relation to the total solid content as a pore former, whereas the slurry used for the membrane layer did not contain any corn starch as

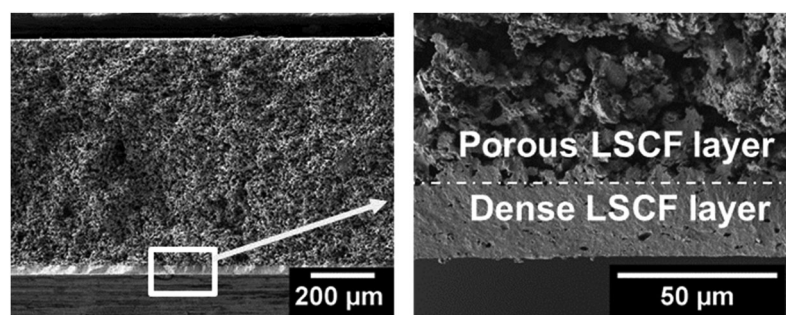


Fig. 20 Cross section of the  $\text{La}_{0.6}\text{Sr}_{0.4}\text{Co}_{0.2}\text{Fe}_{0.8}\text{O}_{3-\delta}$  (LSCF) perovskite membrane developed at FZ Jülich and used in the  $\text{NH}_3$  partial oxidation to  $\text{NO}$ .<sup>73</sup> Reproduced with permission from Wiley-VCH.

a pore former. After sintering at 1100 °C for 3 h in air, the disc membrane consists of a dense top layer of about 70 μm and an 830 μm thick porous support layer with 34% open porosity,<sup>67</sup> as shown in Fig. 18. This membrane has been successfully used in a catalytic membrane reactor for thermal water splitting on the porous support side of the oxygen-transporting BSCF membrane and oxidative coupling of methane to C<sub>2+</sub> hydrocarbons on the dense side of the BSCF membrane.<sup>68</sup>

In the last few years, the sequential tape casting technology at FZ Jülich has been developed and supported membranes with about 20 μm dense BSCF perovskite layers can be prepared (Fig. 19).<sup>69</sup> Such a thin BSCF membrane could be used in a novel concept of the transformation of methane into aromatic fuels and chemicals called methane de-hydro-aromatization.<sup>70</sup>

Another newly developed asymmetric ultrathin perovskite LSCF (La<sub>0.6</sub>Sr<sub>0.4</sub>Co<sub>0.2</sub>Fe<sub>0.8</sub>O<sub>3-δ</sub>) membrane<sup>72</sup> is shown in Fig. 20, a thin (25 μm), dense LSCF layer was supported by a mechanically stable porous LSCF layer of the same chemical composition that was approximately 800 μm thick. The LSCF material was selected as the oxygen-permeable membrane, as it combines high permeability with an intrinsic catalytic activity towards the oxidation of ammonia.

## 4 Conclusions

- Both organic and inorganic hierarchical filter and gas separation membranes usually show a nature-inspired asymmetric or a graded hierarchical cross section. On a coarse support, layers with decreasing pore size are deposited. In the case of gas separation membranes, on top of the hierarchical multi-layer membrane is the gas-selective top layer.

- This hierarchical structure helps to have the pressure drop over the membrane (gas separation) or the transmembrane pressure (particle filtration) as low as possible and ensures high fluxes.

- Inorganic graded or asymmetric membranes as (i) plates and (ii) tubes/capillaries/fibers with a hierarchical wall cross section can be prepared by (i) sequential tape casting, and (ii) the graded asymmetric pore structure is obtained by tuning the parameters of phase inversion spinning or by double mantle spinning.

- In particle filtration applications, the top layer can have a pore size of 100 nm (micro filtration), 10 nm (ultra filtration) or 1 nm (nano filtration). In molecular/atomic gas separation, the top layer on the hierarchical support can be a porous zeolite, a MOF or a carbon film, but also a dense metal or a perovskite film.

- Stacks of ceramic layers with decreasing pore size used in filtration and as supports for gas separation membranes can have very sharp cut-offs in pore size but their manufacture is expensive since each layer has to be fired before the next layer can be coated.

- Zeolite membranes need inorganic supports since usually a structure-directing agent (SDA) has to be removed before by calcination in air at about 500 °C.

- MOF membranes – in contrast – can be activated by a mild treatment to remove occluded solvent molecules. Therefore, MOF layers can be grown on polymeric supports.

- High-temperature oxygen-transporting membranes can be prepared as thin dense layers on a hierarchical porous support of the same chemical composition as the top layer.

## Acknowledgements

JC thanks the European Union Seventh Framework Programme (FP7/2007-2013) under the grant agreement no. 608490 M<sup>4</sup>CO<sub>2</sub> and the Sino German Center for Research promotion (Grant GZ76 and GZ911).

## References

- 1 H. Bux, C. Chmelik, R. Krishna and J. Caro, *J. Membr. Sci.*, 2011, **369**, 284–289.
- 2 <http://biomed.brown.edu>.
- 3 R. Faiz, M. Fallanza, I. Ortiz and K. Li, *Ind. Eng. Chem. Res.*, 2013, **52**, 7918–7929.
- 4 <http://english.nimte.cas.cn>.
- 5 <http://www.gkn.com>.
- 6 M. O. Coppens, *Curr. Opin. Chem. Eng.*, 2012, **1**, 281–289.
- 7 M. O. Coppens, Multiscale nature inspired chemical engineering, in *Multiscale methods – bridging the scales in Science and Engineering*, ed. J. Fish, Oxford University Press, 2009, pp. 536–560.
- 8 <https://Botanistinthekitchen.worldpress.com>.
- 9 <http://www.inopor.com/en/service/information.html>.
- 10 <http://www.gambro.com>.
- 11 X. L. Pan, N. Stroh, H. Brunner, G. X. Xiong and S. S. Sheng, *Sep. Purif. Technol.*, 2003, **32**, 265–270.
- 12 H. Voss, J. Therre, N. Kaltenborn and S. Kaemnitz, *US Pat.*, 8,608,837 B2, 2013.
- 13 W. Schwieger, A. Machoke, A. Inayat, T. Selvam and A. Inayat, *Chem. Soc. Rev.*, 2015, DOI: 10.1039/c5cs00599j.
- 14 S. Thomas, R. Schäfer, J. Caro and A. Seidel-Morgenstern, *Catal. Today*, 2001, **67**, 205–216.
- 15 J. Caro and M. Noack, Zeolite membranes – status and perspective, in *Advances in Nanoporous Materials*, ed. S. Ernst, Elsevier, 2009, p. 58.
- 16 F. H. B. Mertins, H. Kruidhof and H. J. M. Bouwmeester, *J. Am. Ceram. Soc.*, 2005, **88**, 3003–3007.
- 17 K.-H. Kim, S.-J. Cho, K.-J. Yoon, J.-J. Kim, J. Ha and D.-H. Chun, *J. Membr. Sci.*, 2002, **199**, 69–74.
- 18 P. M. Biessheuvel, V. Breedveld, A. P. Higler and H. Verweij, *Chem. Eng. Sci.*, 2001, **56**, 3517–3525.
- 19 Courtesy of Prof. Henning Krieg, School of Chemistry and Biochemistry, North-West University, Potchefstroom, South Africa.
- 20 <http://www.ikts.fraunhofer.de>.
- 21 <http://www.yamit-f.com>.
- 22 B. R. Solomon, M. N. Hyder and K. K. Varanasi, *Sci. Rep.*, 2014, **4**, 5504.

- 23 D. Calamas, J. Baker and M. Sharif, *J. Fluids Eng.*, 2013, **135**, 101202.
- 24 N. Rangnekar, N. Mittal, B. Elyassi, J. Caro and M. Tsapatsis, *Chem. Soc. Rev.*, 2015, **44**, 7128–7154.
- 25 H. Voß, A. Diefenbacher, G. Schuch, H. Richter, I. Voigt, M. Noack and J. Caro, *J. Membr. Sci.*, 2009, **329**, 11–17.
- 26 H. Richter, H. Voß, I. Voigt, A. Diefenbacher, G. Schuch, F. Steinbach and J. Caro, *Sep. Purif. Technol.*, 2010, **72**, 388–394.
- 27 N. Wang, Y. Liu, A. Huang and J. Caro, *Microporous Mesoporous Mater.*, 2015, **207**, 33–38.
- 28 J. Caro and M. Noack, Zeolite membranes – status and prospective, in *Advances in Nanoporous Materials*, ed. S. Ernst, Elsevier, 2009, vol. 1, p. 58.
- 29 G. W. Meindersma and A. B. de Haan, *Desalination*, 2002, **149**, 29–34.
- 30 S. Tennison, *Membr. Technol.*, 2000, **4**, 4–9.
- 31 K.-V. Peinemann, GKSS Geesthacht, Germany, personal information.
- 32 J. Gascon and F. Kapteijn, *Angew. Chem., Int. Ed.*, 2010, **49**, 1530–1532.
- 33 J. C. Tan and A. K. Cheetham, *Chem. Soc. Rev.*, 2011, **40**, 1059–1080.
- 34 G. Ferrey and C. Serre, *Chem. Soc. Rev.*, 2009, **38**, 1380–1399.
- 35 S. R. Venna and M. A. Carreon, *J. Am. Chem. Soc.*, 2010, **132**, 76–78.
- 36 H. Guo, G. Zhu, I. J. Hewitt and S. Qiu, *J. Am. Chem. Soc.*, 2009, **131**, 1646–1647.
- 37 X. Zou, F. Zhang, S. Thomas, G. Zhu, V. Valtchev and S. Mintova, *Chem. – Eur. J.*, 2011, **17**, 12076–12083.
- 38 R. Ranjan and M. Tsapatsis, *Chem. Mater.*, 2009, **21**, 4920–4924.
- 39 Y. Liu, G. Zeng, Y. Pan and Z. Lai, *J. Membr. Sci.*, 2011, **379**, 46–51.
- 40 S. G. Li, J. L. Falconer and R. D. Noble, *Adv. Mater.*, 2006, **18**, 2601–2603.
- 41 J. Van den Bergh, W. Zhu, F. Kapteijn, J. A. Moulijn, K. Yajima, K. Nakayama, T. Tomita and S. Yoshida, *Res. Chem. Intermed.*, 2008, **34**, 467–474.
- 42 Y. S. Li, F. Y. Liang, H. Bux, W. S. Yang and J. Caro, *J. Membr. Sci.*, 2010, **354**, 48–54.
- 43 H. Bux, F. Y. Liang, J. Cravillon, M. Wiebcke and J. Caro, *J. Am. Chem. Soc.*, 2009, **131**, 16000–16001.
- 44 A. Huang, H. Bux, F. Steinbach and J. Caro, *Angew. Chem., Int. Ed.*, 2010, **49**, 4958–4961.
- 45 A. Huang, W. Dou and J. Caro, *J. Am. Chem. Soc.*, 2010, **132**, 15562–15564.
- 46 Y. S. Li, F. Y. Liang, H. Bux, A. Feldhoff, W. S. Yang and J. Caro, *Angew. Chem., Int. Ed.*, 2010, **49**, 548–551.
- 47 C. Cui, Y. Liu, H. Xu, S. Li, W. Zhang, P. Cui and F. Huo, *Small*, 2014, **10**, 3672–3676.
- 48 G. Lu, C. Cui, W. Zhang, Y. Liu and F. Huo, *Chem. – Asian J.*, 2013, **8**, 69–72.
- 49 M. E. Silvestre, M. Franzreb, P. G. Weidler, O. Shekhah and C. Woll, *Adv. Funct. Mater.*, 2013, **23**, 1210–1213.
- 50 M. C. So, S. Jin, H.-J. Son, G. P. Wiederrecht, O. K. Farha and J. T. Hupp, *J. Am. Chem. Soc.*, 2013, **135**, 15698–15701.
- 51 D. Witters, S. Vermeir, R. Puers, B. F. Sels, D. E. De Vos, J. Lammertyn and R. Ameloot, *Chem. Mater.*, 2013, **25**, 1021–1023.
- 52 J. T. Joyce, F. R. Laffir and C. Silien, *J. Phys. Chem. C*, 2013, **117**, 12502–12509.
- 53 D. Y. Lee, E.-K. Kim, C. Y. Shin, D. V. Shinde, W. Lee, N. K. Shrestha, J. K. Lee and S.-H. Han, *RSC Adv.*, 2014, **4**, 12037–12042.
- 54 G. Xu, T. Yamada, K. Otsubo, S. Sakaida and H. Kitagawa, *J. Am. Chem. Soc.*, 2012, **134**, 16524–16527.
- 55 M. Li and M. Dinca, *Chem. Sci.*, 2014, **5**, 107–111.
- 56 I. Hod, W. Bury, D. M. Karlin, P. Deria, C.-W. Kung, M. J. Katz, M. So, B. Klahr, D. Jin, Y.-W. Chung, T. W. Odom, O. K. Farha and J. T. Hupp, *Adv. Mater.*, 2014, **26**, 6295–6300.
- 57 N. Campagnol, E. R. Souza, D. E. De Vos, K. Binnemans and J. Fransaer, *Chem. Commun.*, 2014, **50**, 12545–12547.
- 58 N. Campagnol, T. Van Assche, T. Boudewijns, J. Denayer, K. Binnemans, D. De Vos and J. Fransaer, *J. Mater. Chem. A*, 2013, **1**, 5827–5830.
- 59 W. Liang and D. M. D'Alessandro, *Chem. Commun.*, 2013, **49**, 3706–3708.
- 60 Z.-Q. Li, M. Zhang, B. Liu, C.-Y. Guo and M. Zhou, *Inorg. Chem. Commun.*, 2013, **36**, 241–244.
- 61 J. Yao, D. Dong, D. Li, L. He, G. Xu and H. Wang, *Chem. Commun.*, 2011, **47**, 2559–2561.
- 62 A. J. Brown, J. R. Johnson, M. E. Lydon, W. J. Koros, C. W. Jones and S. Nair, *Angew. Chem., Int. Ed.*, 2012, **124**, 10767–10770.
- 63 H. T. Kwon and H.-K. Jeong, *J. Am. Chem. Soc.*, 2013, **135**, 10763–10768.
- 64 A. J. Brown, N. A. Brunelli, K. Eum, F. Rashidi, J. R. Johnson, W. J. Koros, C. W. Jones and S. Nair, *Science*, 2014, **345**, 72–75.
- 65 D. Zacher, O. Shekhah, C. Wöll and R. A. Fischer, *Chem. Soc. Rev.*, 2009, **38**, 1418–1429.
- 66 H. K. Arslan, O. Shekhah, J. Wohlgemuth, M. Franzreb, R. A. Fischer and C. Wöll, *Adv. Funct. Mater.*, 2011, **21**, 4228–4231.
- 67 S. Baumann, J. M. Serra, M. P. Lobera, S. Escolástico, F. Schulze-Küppers and W. A. Meulenber, *J. Membr. Sci.*, 2011, **377**, 198–205.
- 68 Z. W. Cao, H. Q. Jiang, H. X. Luo, S. Baumann, W. A. Meulenber, H. Voss and J. Caro, *Catal. Today*, 2012, **193**, 2–7.
- 69 F. Schulze-Küppers, S. Baumann, W. A. Meulenber, D. Stöver and H. P. Buchkremer, *J. Membr. Sci.*, 2013, **433**, 121–125.
- 70 Z. W. Cao, H. Q. Jiang, H. X. Luo, S. Baumann, W. A. Meulenber, J. Assmann, L. Mleczko, Y. Liu and J. Caro, *Angew. Chem., Int. Ed.*, 2013, **52**, 13794–13797.
- 71 J. Caro, *Chem. Ing. Tech.*, 2014, **86**, 1901–1905.
- 72 M. Serra, J. Garcia-Fayos, S. Baumann, F. Schulze-Küppers and W. A. Meulenber, *J. Membr. Sci.*, 2013, **447**, 297–305.
- 73 Z. W. Cao, H. Q. Jiang, H. X. Luo, S. Baumann, W. A. Meulenber, H. Voss and J. Caro, *ChemCatChem*, 2014, **6**, 1190–1194.